# A Hybrid Model to Predict the Gyratory Compaction of Hot Mixed Asphalt

Teng Man[1,2]

[1] *Department of Civil, Environmental, and Geo- Engineering, University of Minnesota, Minneapolis, MN 55455, United States*
[2] *Schoole of Engineering, Westlake University, Hangzhou, Zhejiang 310024, China; manteng@westlake.edu.cn*

---

**Abstract**

The compaction of asphalt mixture is crucial to the mechanical properties and the maintenance of the pavement. However, the mix design, which based on the compaction properties, remains largely on empirical data. We found difficulties to relate the aggregate size distribution and the asphalt binder properties to the compaction behavior in both the field and laboratory compaction of asphalt mixtures. In this paper, we would like to propose a simple hybrid model to predict the compaction of asphalt mixtures. In this model, we divided the compaction process into two mechanisms: (i) visco-plastic deformation of an ordered thickly-coated granular assembly, and (ii) the transition from an ordered system to a disordered system due to particle rearrangement. This model could take into account both the viscous properties of the asphalt binder and grain size distributions of the aggregates. Additionally, we suggest to use discrete element method to understand the particle rearrangement during the compaction process. This model is calibrated based on the SuperPave gyratory compaction tests in the pavement lab. In the end, we compared the model results to experimental data to show that this model prediction had a good agreement with the experiments, thus, had great potentials to be implemented to improve the design of asphalt mixtures.

*Keywords:* Hot mixed asphalt, Compaction, Discrete element method, Hybrid model

---

## 1. Introduction

Hot mixed asphalt is ubiquitous in pavement industry. The mechanical properties and durability of asphalt mixtures are largely influenced by the porosity. High porosity usually leads to low strength and high permeability of the moisture [1, 2], while low porosity may result in high temperature sensibility [3, 4]. Thus, we should maintain a reasonable porosity after the compaction process.

In the construction field, we use roller compactorS to compact the asphalt mixtures. During the compaction process, the material is subjected to both normal pressure and shear stress. In the laboratory, to represent the similar volume properties of the field compaction, a variety of laboratory compaction methods have been developed, among which the SuperPave gyratory compactor (SGC) plays an important role in studying the compaction behavior and mechanical properties of asphalt mixtures [5]. In this study, we use the Brovold SuperPave gyratory compactor for the experimental part. The compactor has one cylindrical ring, one top plate to provide gyratory motion, and one bottom plate (pushed by the loading system) to offer constant pressure (Fig. 1 and 2). Usually, the asphalt mixtures will be compacted with a gyratory speed of 30 rpm (or $n = 0.5$ rps) and a pressure of 600 kPa. The gyratory angle is 1.25° (or $\theta = (1.25/180) \times \pi$). We could calculate the average shear rate during compaction as $\dot{\gamma} = 2\pi n\theta \approx 0.07$.

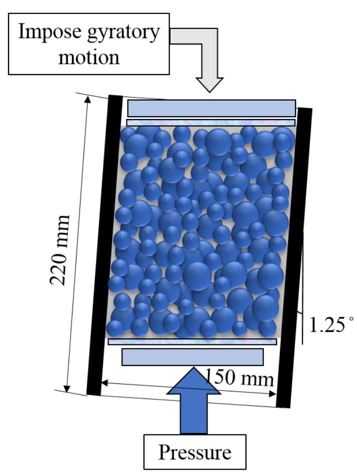


Figure 1: Sketch of the Brovold SuperPave gyratory compactor.

Experimentally, Consuegra et al. [6] compared different laboratory compactors to the field compaction and gave each compactor evaluations based on their ability to produce mixtures with engineering properties similar to those produced in the field, which concluded that the gyratory compactor behaved relatively better than other compaction methods. Also, Hunter et al. [7] analyzed the influence of compaction mode on the mechanical performance of asphalt mixtures. They concluded that both gyratory and vibratory compaction might produce stiffer specimens than the mixtures compacted in the field. To design asphalt mixture using laboratory compactor, Blankenship et al. [8] proposed a rational method for laboratory compaction of hot-mix asphalt. However, even the laboratory compaction process tends to be a random process, and the compaction behavior is governed by a number of factors, such as binder content, binder type, temperature, loading method, aggregates' grain size distributions, aggregate shapes, etc.. Stakston et al. [9] investigated the influence of the angularity of fine aggregates on the compaction behavior of asphalt mixtures, which indicated that a higher fine aggregate angularity may lead to higher resistance to compaction. Delgadillo and Bahia [10], however, analyzed the influence of both temperature and pressure on the behavior of both laboratory and field compaction, and found that the compaction was not reduced dramatically when the temperature was reduced from 125 °C to 75 °C.

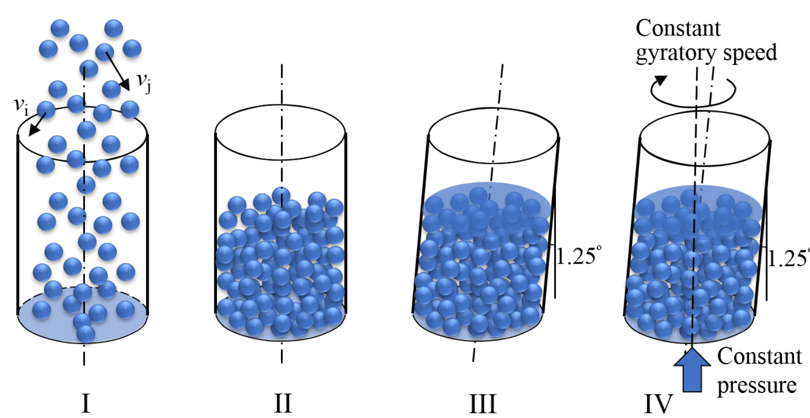


Figure 2: Sketch of the compaction process using Brovold SuperPave gyratory compactor.

While most of the research of the compaction behavior focused on the qualitative analysis of the factors which may influence the gyratory compaction behavior, few research focused on the quantitative investigation of the compaction behavior. Awed et al. [11] proposed a method for predicting the laboratory compaction behavior of asphalt mixtures, which provided us a phenomenological tool for predicting the laboratory compaction. They linked the air void ratio to parameters, such as gradation scale parameter, gradation shape parameter, and asphalt content, and their model also converged to a logarithmic law shown in the following equation [11].

$$AV = a \times [\ln(\mathrm{NG})] + \mathrm{b} \tag{1}$$

where $AV$ is the air void ratio, and $NG$ is the number of gyrations, and $a$ and $b$ are parameters empirically determined by material parameters.

Theoretically, the asphalt mixtures, when in high temperature, can be seen as granular materials (aggregates) with interstitial viscous fluid (asphalt binder) [12]. Thus, the compaction of asphalt mixtures can follow the research of the compaction of granular materials. In the past decades, physicists were interested in the general compaction or relaxation of mono-dispersed or bi-dispersed granular materials [13]. Although the compaction behavior of mono- or bi- dispersed granular materials may differ from the behavior of the compaction of asphalt mixtures, the underlying physics should be similar and transferable. The microscopic analyses of granular materials during compaction induced by tapping or vabrating have been studied [13, 14]. The relationship between collective microscopic structure and the compaction dynamics has been explained [15, 16]. Several equations or models for describing the compaction behavior were proposed based on multiple-time-scale assumption [17, 14, 18]. Among these models, Knight et al. [14] proposed a logarithmic equation to better fit the compaction behavior of mono-dispersed granular materials.

$$\phi(t) = \phi_f - \frac{\Delta\phi_\infty}{1 + B\ln(1 + t/\tau)} \tag{2}$$

where $\phi(t)$ is the volume fraction of granular materials at time $t$, $\phi_f$ is the final volume fraction when time goes to infinity, $\Delta\phi_\infty = \phi_f - \phi_0$ is the difference between $\phi_f$ and the initial volume fraction $\phi_0$, $B$, and $\tau$ are fitting parameters. This form was motivated by, as stated in Ref. [14, 19], the observation of large time intervals of logarithmically slow relaxation in the time evolution of density of the compacted granular materials.

In this paper, we are going to link the compaction of granular materials to the compaction behavior of the asphalt mixtures, at the same time, consider the visco-plastic deformation induced by air voids, viscosity of asphalt binder, and wide grain size distribution. To simplify the analysis of this paper, we consider the asphalt mixture as a mixture of **coarse aggregates** (aggregate with size $> 2.36$ mm) and **fine aggregate mixtures** (FAM, mixture of asphalt binder and fine aggregates). In this study, we will divide the deformation of asphalt mixture during compaction into two parts: (i) the deformation caused by the viscous behavior of FAM, and (ii) the deformation induced the the particle rearrangement. We will organize this paper in the following way. First, after the introduction, we are going to introduce the model framework for prediction the compaction behavior of asphalt mixtures. Then, we will calibrate this model with several experiments obtained in the laboratory. Then, the model will be validated by comparing the modeling results with other experimental results.

## 2. Model Description

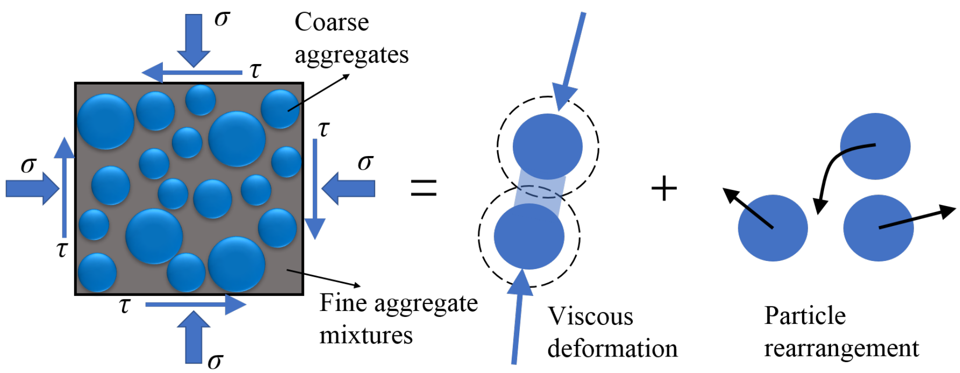


Figure 3: Two parts of the deformation during the compaction of asphalt mixtures: (1) viscous deformation; (2) particle rearrangement.

The motivation of this paper is to understand the compaction behavior of asphalt mixtures from the viewpoint of granular materials. However, as a granular materials, asphalt mixtures are far too complicated because of the complex aggregate shapes and wide range of particle sizes. To tackle such problem, certain simplification is necessary.

- As what we have stated, we divided the asphalt mixture into two parts, one is coarse aggregates (aggregates larger than 2.36 mm), and the other one is fine aggregate matrix (mixture of asphalt binder and fine aggregate ($< 2.36$ mm));

- We consider the coarse aggregates as spherical particles with material properties same as the real aggregates. The median size of coarse aggregates is denoted as $d_{50}^{c}$;

- Then, we may regard the fine aggregate matrix as the thick coatings on the surface of coarse aggregates.

- Meanwhile, the FAM itself is a granular-fluid system with average particle size same as the median particle size of the fine aggregates, $d_{50}^{f}$. The constitutive relationship of the FAM follows the same rule as the rheology proposed by Trulsson et al. in Ref [20].

Firstly, one part of the deformation during the compaction processes comes from the deformation of FAM coatings when two coarse aggregates approach each other. Secondly, as the asphalt mixture approaches random loose packing, the particles would also like to rearrange themselves to form a more stable packing. Then the effect of particle rearrangement will gradually play an important role as the compaction proceed. As we can see from Fig. 3, during the compaction process, we have two types of deformation. Usually at the beginning of the compaction, the FAM serves as coatings of the coarse aggregate, which prevent two adjacent particles from coming toward each other, which brings the viscous deformation of the whole mixture. On the other hand, when the solid fraction of aggregate packing become larger and larger, the particle rearrangement starts to play important roles. The particle will oscillate during compaction, which may create free space for the other particles to move inside, which can help the whole mixture to form a denser state. Thus, we have the following equation:

$$\phi(t) = \phi_v(t) + \Delta\phi_{rp}(t) \tag{3}$$

where $\phi(t)$ is the volume fraction of the asphalt mixture at time $t$, $\phi_v(t)$ is the volume fraction of the asphalt mixture due to viscous deformation at time $t$, and $\Delta\phi_{rp}(t)$ is the change of volume fraction due to rearrangement of particles at time $t$. Here we consider the effect of particle rearrangement as the increment on top of viscous deformations.

We should note that the behavior of the FAM follows the rheology of granular-fluid systems (or slurries) proposed by Trulsson et al in Ref. [20], where the frictional rheology of a granular-fluid system is governed by a dimensionless number, $K = I_v + \alpha I_c^2$, and $I_c = \dot{\gamma} d/\sqrt{\sigma/\rho_p}$ is called the inertial number, and $I_v = \eta\dot{\gamma}/\sigma$ is called the viscous number. Here, $\sigma$ is the normal stress and $\eta$ is the dynamic viscosity of the interstitial fluid. In this section, to build a reasonable model framework, we are going to discuss these two compaction sources.

### *2.1. Visco-plastic deformation induced by the FAM*

To calculate the visco-plastic deformation induced by the FAM, we simplify the asphalt mixture to have a ordered crystal-like structure as it is shown in Fig. 4. The forces acting on two adjacent aggregates can be calculated based on the effective viscosity and thickness of the FAM coatings. Because we use crystal-like structure to simplify the asphalt mixture, the problem become one-dimensional. The fundamental element of the crystal-like structure is shown in Fig. 5.

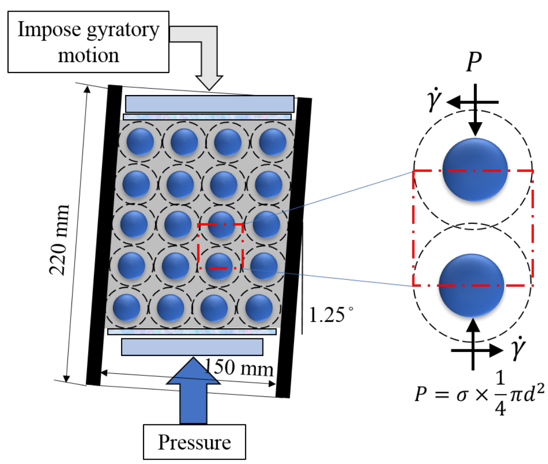


Figure 4: Simplification of the viscous deformation induced by the FAM coatings on the surface of coarse aggregates.

We show that the deformation can be calculated using a computational cell shown in Fig. 5. The problem becomes solving the motion of particle $j$ under pressure $\sigma = 600$ kPa and Shear rate $\dot{\gamma} = 0.07$. The acting loading on the particle $j$ is introduced by the compaction pressure. We have two parts of resistance forces: (1) squeeze-induced lubrication force, and (2) shear-induced resistance forces. Thus, we can obtain the following equations:

$$m\frac{d^2x}{dt^2} = \sigma \times \frac{1}{4}\pi(d_{50}^c)^2 - \eta_{\text{eff}}^n \dot{\gamma} \times \pi\big(G_f R_{\text{eff}}^2\big) - \frac{6\pi\eta_{\text{eff}}^t R_{\text{eff}}^2 G_f^2}{h_0 - x}\frac{dx}{dt} \tag{4a}$$

$$G_f = 1 - \left[1 + \frac{2V_L}{\pi R_{\text{eff}}(h_0 - x)^2}\right]^{-0.5} \tag{4b}$$

where $x$ is the displacement of the particle $j$, $\eta_{\text{eff}}^n$ and $\eta_{\text{eff}}^t$ are the normal and tangential effective viscosities of the FAM, $V_L = 8\delta_c^3$ is the effective volume of FAM between two coarse aggregates, $\delta_c$ is the thickness of the FAM coating, which can be calculated based on the volume ratio between coarse aggregates and the FAM, $G_f$ is the effective coefficient calculated based on the effective volume of FAM, $R_{\text{eff}} = (1/R_i + 1/R_j)^{-1}$ is the effective radius of adjacent particles (Here, $R_i = R_j = 0.5d_{50}^c$). In Fig. 5, $H(t)$ is the distance between centers of two particles at time $t$, and $H_0 = H(t)$ is the initial value of $H$. $h(t)$ is the distance between the surfaces of two particles at time $t$, and $h_0 = h(0)$ is the initial value of $h$.

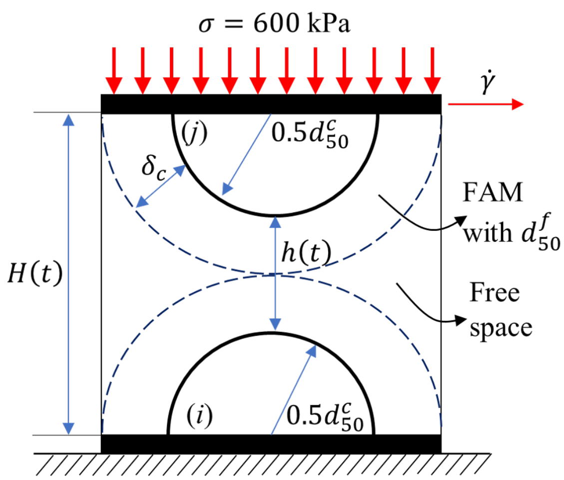


Figure 5: Computational cell for calculating the change of volume fraction due to the viscous deformation of the FAM coatings, based on which we can form the differential equation for calculating the motion of particles so that we could also calculate the volume fraction versus time.

We have stated that the constitutive relationship of the FAM coating follows the rheology of granular-fluid systems proposed in Ref. [20, 12, 21].

Thus, we could first calculate the frictional rheology (effective frictional coefficient, $\mu_{\text{eff}}$, and solid fraction, $\phi_{\text{FAM}}$) of the FAM with the following equations.

$$K = I_v + \alpha I_c^2 \tag{5a}$$

$$\mu_{\text{eff}} = \mu_1 + \frac{\mu_2 - \mu_1}{1 + K_0/\sqrt{K}} \tag{5b}$$

$$\phi_{\text{FAM}} = \frac{\phi_m}{1 + \beta_k \sqrt{K}} \tag{5c}$$

where, according to [12, 21], $\alpha \approx 0.03$, $\mu_1 = 0.265$, $\mu_2 = 2.2$, $K_0 = 0.5$, $\phi_m = 0.605$, $\beta_k = 0.8$ are fitting parameters. We can then calculate the normal and tangential effective viscosities accordingly [21].

$$\eta_{\text{eff}}^t \equiv \frac{\tau}{\dot{\gamma}} = \frac{1}{26\dot{\gamma}} \left[\alpha \rho_p (\dot{\gamma} d)^2 + \eta_b \dot{\gamma}\right] (\phi_m - \phi_s)^{-2.52} \tag{6a}$$

$$\eta_{\text{eff}}^n \equiv \frac{\sigma_n}{\dot{\gamma}} = \frac{\eta_s}{\mu_{\text{eff}}} \tag{6b}$$

where $\eta_b$ is the dynamics viscosity of the asphalt binder at compaction temperature, $\alpha \approx 0.03$ according to Ref. [12], $\mu_1 = 0.265$, $\mu_2 = 2.2$, and $K_0 = 0.5$ are fitting parameters.

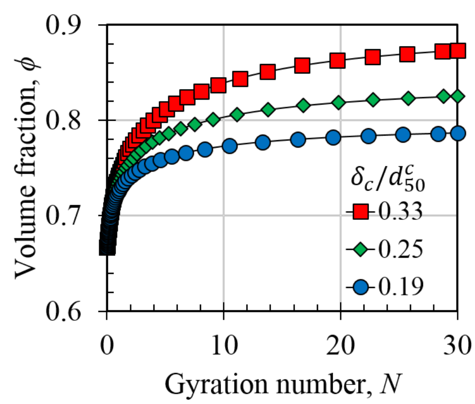


Figure 6: Comparison of the volume fraction / gyration number relationship as we change the thickness of FAM coating.

Based on the rheology of granular-fluid systems proposed by Trulsson et al. [20], we could apply the calculated normal and tangential effective viscosities to the ordinary differential equation in Eqn. 4a, and solve it using

MATLAB internal function **ode45s()**. After calculation we can obtain the relationship between the displacement $x$ and time $t$, then we could convert the displacement to volume fraction of asphalt mixtures and convert the time to gyration numbers ($\phi_{vp} = \phi_{vp}(N)$). To test the results of the ODE, we chose three different coating thickness (three different mass ratio between the FAM and coarse aggregates). Fig. 6 shows the relationship between volume fraction of the ordered asphalt mixtures, $\phi$, and the number of gyrations, $N$. It shows that, as we increase the amount of the FAM (which lead to the increase of FAM coating thickness), the compaction volume fraction can be improved accordingly.

### *2.2. Rearrangement of aggregates*

In the previous section, we could see that, based on the viso-plastic deformation of the FAM coating, the volume fraction of the asphalt mixture could not even reach 90%, this lead us to the next step: to consider the rearrangement of the particles. We approach the problem theoretically with several simplifications in the previous section, but to deal with the particle rearrangement, we have no theoretical tools in hand. Thus, we use discrete element method (DEM) to simulate the gyratory compaction behavior of granular materials with interstitial fluid. However, the asphalt mixtures has wide range of particle sizes, and it is time-consuming to model every particle size in a mixture. Thus, certain assumptions have to be made: (1) The efficiency of particle rearrangement is only governed by the loading conditions (pressure, shear rate, etc.) and particle size distribution; (2) during the compaction process of asphalt mixtures, unlike bi-dispersed surface granular flows, no segregation occurs, which is consistent with the experimental observation of the experiments [22]; (3) The overall particle rearrangement effect of different sizes can be summed up based on the mixture theory; (4) The compaction of each size group of particles is governed by the mean size of this size group.

Based on these assumptions, we can use discrete element method (DEM) to simulate the gyratory compaction of a monodispersed granular-fluid system in a SuperPave gyratory compactor configuration shown in Fig. 1. We compacted the granular materials with particle diameters = $(2 \pm 0.4)$ mm using constant pressure of 600 kPa, gyratory speed of 30 rpm, gyratory angle of $1.25°$, and the viscosity of the interstitial fluid is set to be equal to 250 cP. To simplify the analyses, we neglected the effect of interstitial fluid on the particle rearrangement. All the dimensional parameters will be normalized using

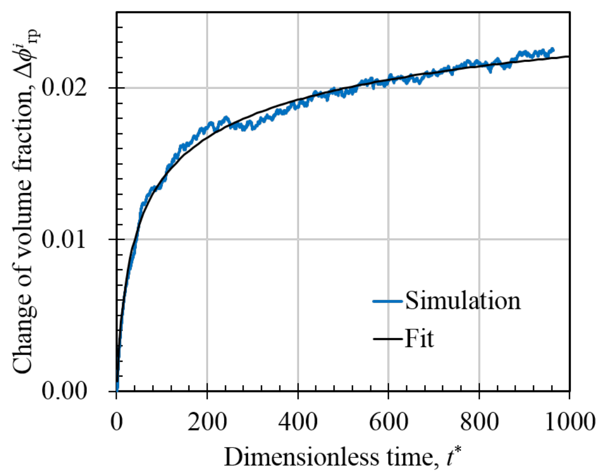


Figure 7: Relationship between the solid fraction of particle rearrangement and the dimensionless time, $t^*$

average particle radius, $\bar{r}_p$, mass of average-size particles, $\bar{m} = (4/3)\pi\bar{r}_p^3\rho_p$, and gravitational acceleration, $g$. Thus, the compaction time, $t$ can be non-dimensionalized as $t^* \equiv t\sqrt{g/\bar{r}_p}$, where $t^*$ is the dimensionless time. In Fig. 7, we plotted the relationship between dimensionless time, $t^*$, and the change of solid fraction of granular materials during the compaction. Here, the change of solid fraction can be seen as the effect of particle rearrangement. The compaction curve in Fig. 7 can be fitted with the following equation:

$$\Delta\phi^i_{rp}(t^*) = 0.052 - \frac{0.052}{1 + 0.17\ln\left(1 + \frac{t^*}{\tau}\right)} \tag{7}$$

where $\Delta\phi^i_{rp}(t^*)$ is the change of volume fraction for a compaction of particles with certain average grain size, $t^*$ is the dimensionless time. This fitting curve is based on Eq. 2.

The above fitting curve can only be used to quantify a monodisperse granular assembly. To obtain the total effect of particle rearrangement of the whole grain size distribution, we have be implement mixture theory. We divide the aggregates into different size groups based on the sieving test. Each size group of aggregates is bounded by adjacent sieve sizes ($d_i$ and $d_{i+1}$), and the mean size of each size group is calculated by $\bar{d}_i = \sqrt{d_i d_{i+1}}$ and $\bar{r}^i_p = 0.5\bar{d}_i$. On one hand, based on the mean size of each size group, we can calculate the compaction behavior of each size group, $\Delta\phi^i_{rp}(t^*)$, where

$t^*$ is a function of particle size. On the other hand, we can also obtain the mass ratio of each size group based on the sieving test, $\Psi_i$. Then, we obtain the total particle rearrangement effect based on the grain size distribution of aggregates.

$$\Delta\phi_{rp}(t) = \Sigma_{i=1}^{N_s}\left[\Psi_i \Delta\phi_{rp}^i(t)\right] \tag{8}$$

where $N_s$ is the number of aggregate size groups in the sieving test.

### 2.3. Redistribution of particle rearrangement

In previous sections, we analyzed the contributions of both viscous deformation and particle rearrangement to the overall compaction process. In this process, we treated the viscous contribution as the foundation of the change of solid fraction, and regarded the particle rearrangement effect as the increment. However, due to the existence of the viscous effect, the particle rearrangement may not happen in the same way as we have calculated, thus, the two part of contributions cannot be added together directly. In this section, we proposed a redistribution function of particle rearrangement to reshape the the curve of $\Delta\phi_{rp}(t)$.

The basic idea is that at the beginning of the compaction, due to the huge effect of viscous deformation stated in the previous section, the effect of particle rearrangement is smaller that what we had in the DEM simulations. Thus, we would like to decrease the influence of particle rearrangement at the beginning of the compaction, but enhance the influence of that toward the end of the compaction. We proposed the following equation to capture the redistribution of the particle rearrangement.

$$\xi_{rp}(N) = 0.5 + \frac{1}{1 + \tau_{rp}/N} \tag{9}$$

where $\tau_{rp}$ is the balancing point, which depend on the grain size distribution, and $N$ is the gyration number. Once we know the viscosity of asphalt binder at the compaction temperature and the grain size distribution of the aggregate, the relationship between $\tau_{rp}$ and the grain size distribution is the only parameter we need to calibrate. In the end, if we combine the contributions from both the viscous deformation and the particle rearrangement, we can obtain the following relationship between volume fraction of asphalt mixtures, $\phi_{vf}$, and the compaction time, $t$, to describe the whole gyratory compaction process of asphalt mixtures:

$$\phi_{vf}(t) = \phi_{vp}(t) + \xi_{rp}(N(t))\Delta\phi_{rp}(t) \tag{10}$$

## 3. Model Calibration

The model we proposed require the information of the viscosity of asphalt binder, and the sieving analysis results of the aggregates, based on which we could obtain both the viscous deformation and the particle rearrangement effect during the compaction process of the asphalt mixtures. However, since we also need to redistribute the particle rearrangement effect, the parameter, $\tau_{rp}$, needs to be calibrated using experimental study. In this section, we are going to provide such experimental results to obtain a reasonable value of this parameter.

### *3.1. Materials and experimental work*

In this study, the main point is to capture the influence of aggregate grain size distributions, thus we prepared seven sets of compaction experiments with different grain size distribution to calibrate the redistribution of the particle rearrangement effect. In these experiments, we use the same type of asphalt binder (PG64-22). No additives were added to the asphalt binder. As what we have stated, in the analysis of viscous deformation, we treat the asphalt binder as a Newtonian fluid with viscosity measured at 135°C and 20 rpm. We measured the viscosity at such temperature and rotational speed using a rotational viscometer, and obtained that the viscosity of asphalt binder is approximately 250 cP.

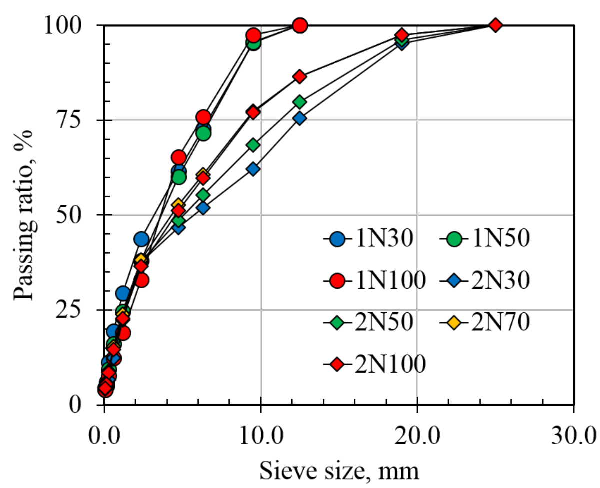


Figure 8: Grain size distribution of aggregates.

We acquired the aggregate from two sources: river sand and quarry gravels. We show the size distribution of the seven sets of aggregates in Fig. 8. Four sets of aggregate has maximum diameter of 12.5 mm, while three sets of aggregate has maximum diameter of 25 mm. During the experiment, we first put all the materials into the oven, which set to be at 140°C. After remaining in the oven for one hour, the materials were transferred to the mixer to be mixed for 180 seconds. To compact the asphalt mixtures in a laboratory, we used Brovold SuperPave gyratory compactor (Fig. 1). This experimental apparatus can compaction the asphalt mixtures at constant pressure and constant shear rate. Following the standard compaction testing procedure [23], we set the compaction pressure at 600 kPa, gyratory angle at 1.25°, and gyratory speed at 30 rpm.

The height of the mixture was measured after each gyration. In order to calculate the volume fraction of the asphalt mixture at each gyration number based on the position of the bottom plate of the compactor, we also need to measure both the the theoretical maximum specific gravity, $G_{mm}$, and the bulk specific gravity of the mix, $G_{mb}$, which were conducted based on ASTM D2041 and ASTM D2726 [24, 25]. Based on the recorded position of the bottom plate, and the measured $G_{mm}$ and $G_{mb}$, the volume fraction ($\phi_{\text{mix}} = 1 - \phi_{\text{air}}$, where $\phi_{\text{mix}}$ was the volume fraction of the compacted asphalt mixture, and $\phi_{\text{air}}$ was the air void ratio of the compacted asphalt mixture) can be calculated in the software attached to the SuperPave gyratory compactor. The relationship between $\phi_{\text{mix}}$ and the gyration number can be obtained accordingly.

### *3.2. Experimental results and model calibration*

The markers with different colors in Fig. 8 show the experimental results with different grain size distributions. It shows that the compaction behavior can be greatly influenced by the grain size distribution of aggregates. By comparing the experimental results with the characteristic parameters of the grain size distributions (mass ratio between fine aggregates and coarse aggregates, median aggregate sizes, etc.), we could conclude that more fine aggregates and smaller median aggregate size could result in better compaction results.

As what we have stated, we would like to find the relationship between the balancing point, $\tau_{rp}$, and the grain size distrbution for the model calibration. Thus, we first obtained the best fit (with a specific $\tau_{rp}$) for each experimental results, plotted as solid curves with different colors (Fig. 9). Then, we plotted

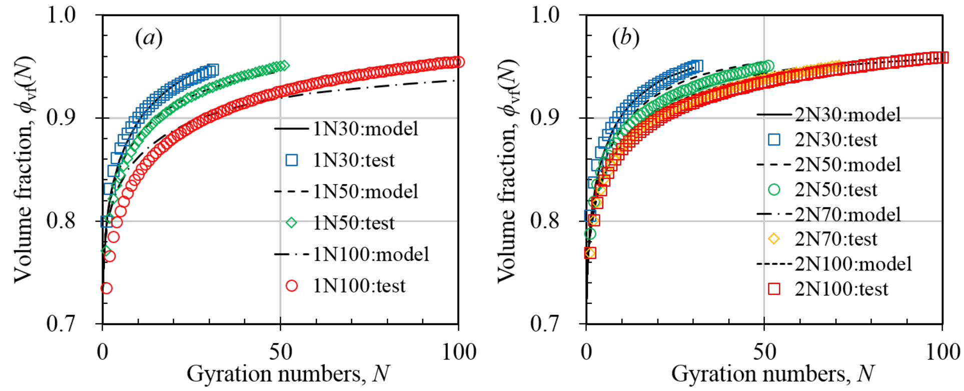


Figure 9: Comparison between experimental results and the results obtained from the proposed hybrid model

the fitted balance point, $\tau_{rp}$, against the median aggregate size (radius), $r_{50}$ (Fig. 10). We found that the relationship between $\tau_{rp}$ and $d_{50}$ can be described usingn the following parabolic equation:

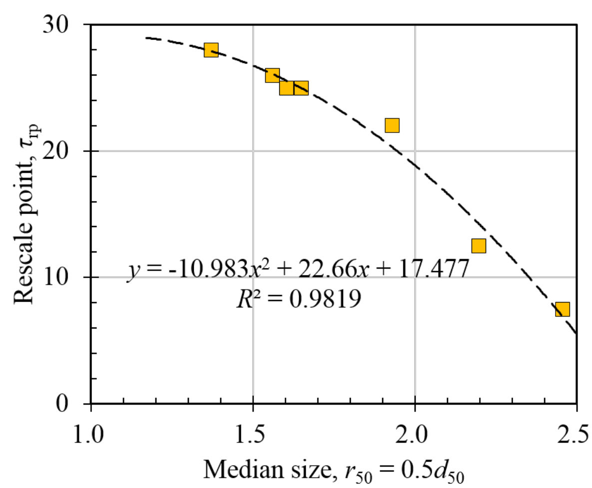


Figure 10: The relationship between $\tau_{rp}$ and median radius $r_{50}$

Thus, we have associated each part of the compaction contribution to the properties of asphalt binder and the grain size distributions. The calibrated model could be used to predict the gyratory compaction behavior of asphalt mixtures in the future.

Table 1: Mix design of the model validation experiments

| Sieve size (mm) | 3N30 (%) | 3N50 (%) | 3N100 (%) |
|---|---|---|---|
| 12.5 | 100 | 100 | 100 |
| 9.5 | 94.1 | 94.7 | 95.3 |
| 6.3 | 71.5 | 72.2 | 72.9 |
| 4.75 | 60.5 | 61.3 | 62.0 |
| 2.36 | 42.4 | 38.2 | 34.0 |
| 1.18 | 29.2 | 24.9 | 20.4 |
| 0.60 | 19.7 | 16.4 | 12.8 |
| 0.30 | 11.5 | 9.9 | 7.6 |
| 0.15 | 6.1 | 5.7 | 4.2 |
| 0.075 | 4.6 | 4.3 | 3.0 |
| $r_{50}$ (mm) | 1.41 | 1.54 | 1.68 |
| $\tau_{rp}$ | 27.6 | 26.3 | 24.4 |

## 4. Model validation and discussions

This model can be validated with a set of different compaction experiments (3N30, 3N50, 3N100). The maximum aggregates size of this set of experiments is 12.5 mm. The overall size distributions is shown in Table 1. It shows that three different compaction tests have different grain size distributions, different percentage of fine aggregate mixtures, different median radius, and different balance point of the particle rearrangement. Based on the material information, we could implement the model we introduced in previous sections. The model can be validated if the model prediction matches the experimental results.

In Fig. 11, we showed both the experimental results (markers) and the model predictions (lines). Generally, the prediction has great agreement with the experimental results, which indicates that this simple model could roughly capture the compaction behavior of hot mixed asphalt.

Besides, this model could help us with the understanding of the compaction mechanism of asphalt mixtures. Previously, we would regard the compaction deformation of asphalt mixtures as the result of the squeeze of

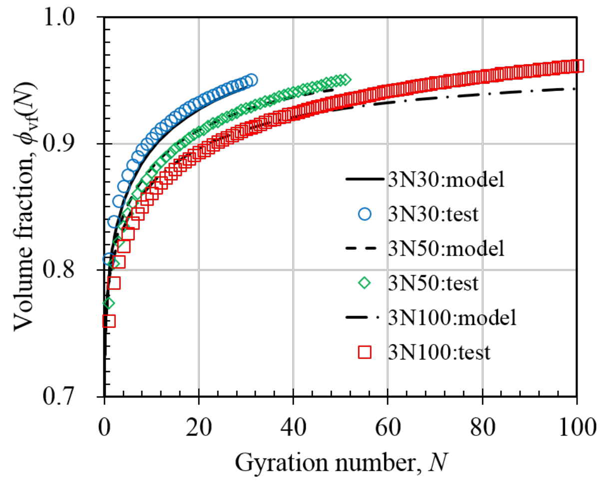


Figure 11: Results of model validations

air voids in porous media, thus simulate the process using the porous media mechanical models. In our model, we reverse the thinking and, instead of investigating the deformation brought by the change of air voids, we put priority on the solid-fluid mixture itself.

This model confirms the importance of the grain size distribution of aggregates on the compaction results. With this model, we could find that increasing the mass of fine aggregate matrix could help improve the compaction efficiency by influencing the visco-plastic deformations during compaction process. Also, a reasonable grain size distribution could also benefit the particle rearrangement effect. Meanwhile, we should acknowledge that such model is still relatively preliminary, thus need more experimental data to calibrate and validate.

## 5. Conclusions

This paper provides a simple hybrid model for predicting the compaction behavior of asphalt mixture in a SuperPave gyratory compactor. Different from previous phenomelogical model where the compaction curves were fitted using different forms of equations and continuum models considering the compaction as the deformation of air voids, the author divided the compaction deformation into two parts: (1) viscous deformation due to the existence of asphalt binder; (2) particle rearrangement due to the compaction excitation.

The viscous deformation can be solved numerically based on a theoretical differential equation, while the particle rearrangement effect can be quantified based on DEM simulation of monodisperse granular materials and mixture theory. Based on experimental results, this model can be calibrated and further validated.

Although being preliminary, this method did bring a relatively functional tool for predicting the gyratory compaction process of asphalt mixtures. With this model, we could calculate the compaction deformation based on the mix design of asphalt mixtures, which could be both time-saving and economical for the pavement industry. Furthermore, such model has potentials to be improved with more experimental data so that it can be applied to predict the field compaction of asphalt mixtures.

## 6. Acknowledgement

The author of this paper would like to acknowledge the help from Prof. Kimberly Hill and Prof. Jia-Liang Le for the discussions about the model framework. The author would also thank the Saint Anthony Fall Laboratory at UMN for the computing resources provided.

## References

[1] E. Zube, Compaction studies of asphalt concrete pavement as related to the water permeability test, Highway Research Board Bulletin (1962).

[2] L. Santucci, D. Allen, R. Coats, The effects of moisture and compaction on the quality of asphalt pavements, in: Proceedings of Association of Asphalt Paving Technologists, volume 54, pp. 168–208.

[3] G. Huber, G. Heiman, Effect of asphalt concrete parameters on rutting performance: A field investigation (with discussion), in: Association of Asphalt Paving Technologists Proc, volume 56.

[4] M. C. Ford Jr, M. C. Ford Jr, Pavement densification related to asphalt mix characteristics, 1178, 1988.

[5] R. B. Mallick, Use of superpave gyratory compactor to characterize hot-mix asphalt, Transportation Research Record 1681 (1999) 86–96.

[6] A. E. Consuegra, D. N. Little, H. Von Quintus, J. Burati, Comparative evaluation of laboratory compaction devices based on their ability to produce mixtures with engineering properties similar to those produced in the field, Master's thesis, Texas A&M University, 1988.

[7] A. E. Hunter, L. McGreavy, G. D. Airey, Effect of compaction mode on the mechanical performance and variability of asphalt mixtures, Journal of Transportation Engineering 135 (2009) 839–851.

[8] P. B. Blankenship, K. C. Mahboub, G. A. Huber, Rational method for laboratory compaction of hot-mix asphalt (with discussion and closure), Transportation Research Record (1994).

[9] A. D. Stakston, H. U. Bahia, J. J. Bushek, Effect of fine aggregate angularity on compaction and shearing resistance of asphalt mixtures, Transportation Research Record 1789 (2002) 14–24.

[10] R. Delgadillo, H. U. Bahia, Effects of temperature and pressure on hot mixed asphalt compaction: field and laboratory study, Journal of materials in civil engineering 20 (2008) 440–448.

[11] A. Awed, E. Kassem, E. Masad, D. Little, Method for predicting the laboratory compaction behavior of asphalt mixtures, Journal of Materials in Civil Engineering 27 (2015) 04015016.

[12] T. Man, Q. Feng, K. Hill, Rheology of thickly-coated granular-fluid systems, arXiv preprint arXiv:1812.07083 (2018).

[13] A. Mehta, G. Barker, The dynamics of sand, Reports on Progress in Physics 57 (1994) 383.

[14] J. B. Knight, C. G. Fandrich, C. N. Lau, H. M. Jaeger, S. R. Nagel, Density relaxation in a vibrated granular material, Physical review E 51 (1995) 3957.

[15] O. Pouliquen, M. Belzons, M. Nicolas, Fluctuating particle motion during shear induced granular compaction, Physical review letters 91 (2003) 014301.

[16] A. Mehta, G. Barker, J. Luck, Cooperativity in sandpiles: statistics of bridge geometries, Journal of Statistical Mechanics: Theory and Experiment 2004 (2004) P10014.

[17] G. Barker, A. Mehta, Transient phenomena, self-diffusion, and orientational effects in vibrated powders, Physical Review E 47 (1993) 184.

[18] P. Philippe, D. Bideau, Compaction dynamics of a granular medium under vertical tapping, EPL (Europhysics Letters) 60 (2002) 677.

[19] E. R. Nowak, J. B. Knight, E. Ben-Naim, H. M. Jaeger, S. R. Nagel, Density fluctuations in vibrated granular materials, Physical Review E 57 (1998) 1971.

[20] M. Trulsson, B. Andreotti, P. Claudin, Transition from the viscous to inertial regime in dense suspensions, Physical review letters 109 (2012) 118305.

[21] T. Man, Rheology of granular-fluid systems and its application in the compaction of asphalt mixtures, Ph.D. thesis, University of Minnesota - Twin Cities, 2019.

[22] E. Brown, R. Collins, J. Brownfield, Investigation of segregation of asphalt mixtures in the state of georgia, Transportation Research Record (1989).

[23] ASTM/D6925-15, Standard test method for preparation and determination of the relative density of asphalt mix specimens by means of the superpave gyratory compactor, American Society for Testing and Materials West Conshohocken, PA.

[24] ASTM/D2041-11, Standard test method for theoretical maximum specific gravity and density of bituminous paving mixtures, American Society for Testing and Materials West Conshohocken, PA.

[25] ASTM/D2726-17, Standard test method for bulk specific gravity and density of non-absorptive compacted asphalt mixtures, American Society for Testing and Materials West Conshohocken, PA.